Published in final edited form as:
Behav Brain Res. 2010 April 2; 208(2): 415–424. doi:10.1016/j.bbr.2009.12.015.

Cognitive Recovery in the Aged Rat after Stroke and Anti-Nogo-A Immunotherapy

Rebecca L. Gillani, BS[1,2,3,*], **Shih-Yen Tsai, MD, PhD**[3], **Douglas G. Wallace, PhD**[4], **Timothy E. O'Brien, PhD**[5], **Ebinehita Arhebamen, MD**[6], **Mateo Tole, BS**[3], **Martin E. Schwab, PhD**[7], and **Gwendolyn L. Kartje, MD, PhD**[1,3,8,9,10]

[1]Neuroscience Program Loyola University Chicago 2160 S. First Avenue Maywood, IL, USA 60153 [2]Stritch School of Medicine Loyola University Chicago 2160 S. First Avenue Maywood, IL, USA 60153 [3]Research Service Hines VA Hospital 5000 S. Fifth Avenue Hines, IL, USA 60141 [4]Dept. of Psychology Northern Illinois University Psychology-Computer Science Building De Kalb, IL, USA 60115 [5]Dept. of Mathematics and Statistics Loyola University Chicago 6525 N. Sheridan Road Chicago, IL, USA 60626 [6]Dept. of Medicine Loyola University Chicago 2160 S. First Avenue Maywood, IL, USA 60153 [7]Brain Research Institute University of Zurich and Department of Biology Swiss Federal Institute of Technology Winterthurerstrasse 190, 8057 Zurich Switzerland [8]Dept. of Molecular Pharmacology and Therapeutics Loyola University Chicago 2160 S. First Avenue Maywood, IL, USA 60153 [9]Dept. of Neurology Loyola University Chicago 2160 S. First Avenue Maywood, IL, USA 60153 [10]Neurology Service Hines VA Hospital 5000 S. Fifth Avenue Hines, IL, USA 60141

Abstract

We have previously shown that immunotherapy directed against the protein Nogo-A leads to recovery on a skilled forelimb reaching task in rats after sensorimotor cortex stroke, which correlated with axonal and dendritic plasticity. Here we investigated anti-Nogo-A immunotherapy as an intervention to improve performance on a spatial memory task in aged rats after stroke, and whether cognitive recovery was correlated with structural plasticity. Aged rats underwent a unilateral distal permanent middle cerebral artery occlusion and one week later were treated with an anti-Nogo-A or control antibody. Nine weeks post-stroke, treated rats and normal aged rats were tested on the Morris water maze task. Following testing rats were sacrificed and brains processed for the Golgi-Cox method. Hippocampal CA3 and CA1 pyramidal and dentate gyrus granule cells were examined for dendritic length and number of branch segments, and CA3 and CA1 pyramidal cells were examined for spine density and morphology. Anti-Nogo-A immunotherapy given one week following stroke in aged rats improved performance on the reference memory portion of the Morris water maze task. However, this improved performance was not correlated with structural changes in the hippocampal neurons examined. Our finding of improved performance on the Morris water maze in aged rats after stroke and treatment with anti-Nogo-A immunotherapy demonstrates the promising therapeutic potential for anti-Nogo-A immunotherapy to treat cognitive deficits after stroke. The identification

*(*Corresponding Author)* Research Service 151 Building 1 Hines VA Hospital 5000 S. Fifth Avenue Hines, IL, USA 60141 Telephone : 630-337-9145 resmith@lumc.edu.

of sites of axonal and dendritic plasticity in the aged brain after stroke and treatment with anti-Nogo-A immunotherapy is still under investigation.

Keywords

Nogo-A; Stroke; Aging; Navigation; Dendritic arborization; Dendritic spine

Introduction

Each year 795,000 people in the United States have a new or recurrent stroke, and 87% of these events are caused by blockage of a cerebral artery [27] leading to ischemic brain damage. Such brain damage often results in long-term neurological deficits in various functions including cognition. The risk of stroke increases with age [27], and in the elderly population more advanced age is associated with greater disability after ischemic stroke [21]. This is thought to be due at least in part to the differential response of the aged brain to ischemia, including increased neuronal degeneration and apoptosis [36], faster onset of inflammation and scar formation [3], and increased DNA damage and oxidative stress [25,for review see 37]. Therefore, in order to best investigate the therapeutic potential of emerging therapies for stroke recovery, using the appropriate age group in animal models of stroke is important and recommended by the Stroke Therapy Academic Industry Roundtable (STAIR) [1] and the Stroke Progress Review Group [19].

Spontaneous recovery of function after stroke is thought to be limited by the growth inhibitory environment in the adult CNS which includes the myelin-associated inhibitors [17]. The potent myelin inhibitor Nogo-A was first identified as a neurite growth inhibitory protein *in vitro* [8-10,18,38] and then as an inhibitor of axonal regeneration and compensatory growth and recovery of function in models of spinal cord injury [17]. Subsequently we have shown that anti-Nogo-A immunotherapy after focal ischemic stroke leads to functional recovery in a skilled sensorimotor test in adult and aged rats [30,33,40,41]. The functional recovery in adult rats was correlated with axonal compensatory growth [30,33,40], and increased dendritic arborization and spine density in the contralesional sensorimotor cortex [34], indicating that recovery of sensorimotor function after cortical injury may be achieved by dis-inhibiting sprouting in axons and dendrites by strategies to neutralize the Nogo-A protein.

Importantly, ischemic stroke can lead to other types of neurologic deficits other than sensorimotor impairment, including cognitive disorders. Therefore, we investigated the therapeutic potential of anti-Nogo-A immunotherapy on cognitive recovery after ischemic stroke in aged animals. We found that anti-Nogo-A immunotherapy given one week after stroke in aged rats improved performance on a spatial memory task, but was not correlated with increased dendritic complexity or increased spine density in hippocampal neurons.

Materials and Methods

Animal Subjects

Experiments were approved by the Institutional Animal Care and Use Committee of Hines Veterans Affairs Hospital. Aged male Long Evans black-hooded rats (18 months of age at start of the study) were divided into three groups: (1) Normal aged (n=10), (2) middle cerebral artery occlusion (MCAO)/control antibody treatment (n=13), and (3) MCAO/anti-Nogo-A antibody treatment (n=12).

Stroke Surgery

MCAO was performed as in our previous work [30,33,34,40,41]. Briefly, rats were anesthetized with isoflurane inhalant anesthesia (3% in oxygen). The right MCA was ligated with a 10-0 suture and transected above the suture with microscissors. The right common carotid artery was permanently ligated and the left common carotid artery was temporarily occluded for 60 minutes. Body temperature was maintained throughout the surgery with a heat pad.

Antibody Intracerebroventricular Infusion

The experimental design is depicted in Fig. 1A. One week post-stroke, rats were randomized and anesthetized with isoflurane inhalant anesthesia (3% in oxygen). A cannula was placed into the right lateral cerebral ventricle at coordinates 1.3 mm lateral, 0.8 mm posterior, and 3.8 mm ventral (relative to bregma). An Alzet osmotic minipump (model 2ML2; Durect Corporation, Cupertino, CA, USA) was implanted subcutaneously posterior to the scapulae and connected to the cannula with polyethylene tubing. Either purified mouse monoclonal anti-Nogo-A antibody (11C7, IgG1) or control antibody (anti-wheat auxin, IgG1) was infused at a rate of 12.5 μg/hr (2.5 mg/ml) for two weeks as in our previous work [30] and as first described by Wiessner et al. 2003 [42].

Morris Water Maze

Morris water maze testing started 9 weeks post-stroke. This time-point of was chosen based upon our previous work which showed that aged rats treated with anti-Nogo-A immunotherapy 1 week post-stroke had significantly improved sensorimotor function starting at 9 weeks post-stroke [30]. Experimenters were blinded to antibody treatment and prominent distal cues throughout the room remained constant throughout testing.

PLACE TASK—During days 1-7 of testing the hidden platform (4×4 inches) was always located in the same position in the pool (6 feet in diameter). Rats were given four trials per day, separated by at least 5 minutes, starting from each of the four cardinal locations in a random order. When rats reached the platform, they were allowed to remain there for 30 seconds, and then removed. The place task evaluates the rats' ability to learn about the environmental cues to guide movement toward the hidden platform.

PROBE TRIAL—On day 8 of testing the platform was removed from the pool and the rats were given one probe trial lasting 2 minutes. The probe trial tests whether the rats prefer the pool quadrant where the platform was previously located during the place task.

MATCHING-TO-PLACE TASK—On days 9-13 of testing the platform location was moved each day. Rats were given two trials per day and trials were separated by 20 seconds. Rats remained on the platform for 30 seconds. The matching-to-place task evaluates the rats' ability to update their representations of the hidden platform.

Behavioral Analysis

All water maze trials were recorded to DVD using an overhead bullet camera. Ethovision 3.1 (Noldus Information Technology, Leesbug, VA, USA) video tracking software was used to digitize the trials.

PLACE TASK—Both time and distance to locate the platform from each of the four trials per day were averaged for statistical analysis.

PROBE PREFERENCE SCORE—For the probe trials the probe preference score was calculated as [(T-A)+(T-B)+(T-C)]/3, where T is the swim time in the quadrant that contained the platform during the place task and A, B, and C are the swim times in the other three quadrants [6].

THIGMOTAXIS—Swim times in the outer 50% of the pool were generated from Ethovision 3.1 software for each rat on each of the four trials on seven days of hidden platform testing. A value for thigmotaxis was calculated as swim time in the outer 50 % of the pool over total swim time.

PATH CIRCUITY—Path circuity was calculated as the direct distance to the platform over the total distance traveled to the platform.

Golgi-Cox staining

Thirteen weeks post-stroke and two weeks after completion of Morris water maze testing, rats were overdosed with pentobarbital (100 mg/kg, i.p.) and transcardially perfused with 0.9% saline and 10,000 U heparin/liter. The brains were removed and immersed whole in Golgi-Cox solution [16] for two weeks. The brains were coronally sectioned at 200 μm on a vibratome, mounted on 2% gelatinized slide and reacted as described by Gibb and Kolb [15]. Slides were coded to blind the experimenters to the antibody treatment group.

Stroke Size Analysis

Golgi-Cox stained coronal brain sections were traced using Neurolucida software (mbf Bioscience, Williston, VT, USA) and with the aid of an atlas [35]. Stroke size was represented as percent of the intact contralateral hemispheric area (total area of the intact contralateral hemisphere minus total area of the intact ipsilesional hemisphere over total area of the intact contralateral hemisphere).

Neuroanatomical Analysis

Golgi-Cox stained hippocampal CA3 and CA1 pyramidal cells and dentate gyrus granule cells were analyzed in the dorsal hippocampus as described below.

For illustration purposes, images of representative CA3 and CA1 pyramidal cells and dentate gyrus granule cells were taken. Image stacks were acquired every 5 μm for 130 μm using Neurolucida software, and then a minimum intensity z projection was generated using NIH ImageJ software.

DENDRITIC BRANCHING AND LENGTH—An average of four apical and basilar dendritic trees of CA3 and CA1 pyramidal cells, and dendritic trees of dentate gyrus granule cells were traced for each side of the hippocampus using Neurolucida software and Leica DM 4000 B with a 63x objective. For inclusion neurons had to be well impregnated, unobstructed by other neurons or glial cells, and intact. Dendritic trees were analyzed for dendritic length and number of branch segments using the branched structure analysis tool of Neurolucida. For CA3 and CA1 pyramidal cells, branches originating from the cell body (basilar) or the apical shaft were considered first order, and the next bifurcating branches were considered second order and so on. For dentate gyrus granule cells, branches originating from the cell body were considered first order, and the next bifurcating branches were considered second order and so on. For CA3 analysis 9 brains from each group were analyzed, and for CA1 and dentate gyrus analysis all brains from each group were analyzed.

SPINE DENSITY AND MORPHOLOGY—Four CA3 and CA1 pyramidal cell apical dendritic terminal branches of second or higher order were analyzed for each side of the

hippocampus using a 100x oil immersion lens. For a 50 μm length segment of the branch dendritic protrusions were counted and assigned to a morphology category of filopodium, 2-headed, stubby, thin, and mushroom shaped as described by Bourne and Harris [4]. The first 10 μm of the dendrite after the branch point and the terminal 10 μm were excluded from analysis. For CA3 analysis 9 brains from each group were analyzed, and for CA1 analysis 9 brains from the normal aged group were analyzed, 9 from the stroke/control antibody group, and 8 from the stroke/anti-Nogo-A antibody group.

Statistical Analysis

P values of less than 0.05 were considered significant.

BEHAVIORAL DATA—For comparison of place task time and distance to the platform we started with a general linear model repeated measures ANOVA (SPSS, Chicago, IL, USA). The results from this analysis are presented in Supp. Fig. 1. When we examined plots of time and distance to the platform over the seven days of the place task for each of the rats, we saw a trend for normal aged rats and stroke/anti-Nogo-A antibody rats to have steeper slopes than stroke/control antibody rats. To determine if there were statistically significant differences in the slopes we used a non-linear mixed model in which a y intercept and slope parameter were determined for each individual rat, which has previously been used for rodent behavioral analysis [28]. Specifically for this analysis we used a likelihood based $\chi 2$ test of random-effects simple exponential two-parameter model, $\eta(x) = \theta_1 e^{-\theta_2 x}$, where x = day – 1 [11,20] using SAS software (SAS Institute, Cary, NC, USA). This model was able to identify more subtle differences in performance on the Morris water maze in aged rats, which have greater variability in Morris water maze testing.

For comparison of swim velocities we used a repeated measure ANOVA using SAS software. For comparison of probe preference scores and platform crossings we used a one-way ANOVA using SigmaStat (Systat, San Jose, CA, USA). For comparison of the matching-to-place task times to swim to the platform we used a one-way ANOVA to compare groups separately by trial, and a two-way repeated measures ANOVA to compare groups separately by trial across days using SAS software. For comparison of thigmotaxis we used a likelihood based $\chi 2$ test of random-effects simple exponential three-parameter model, $\eta(x) = \theta_1 e^{-\theta_2 x} + \theta_3$, where x = day – 1 using SAS software. For comparison of the path circuity for the place task we used a repeated measures ANOVA followed by a Bonferroni post-hoc test using the SPSS software.

NEUROANATOMICAL DATA—Neuroanatomical data analysis was performed with SigmaStat as follows: a t-test for stroke size, a one-way ANOVA with Student-Newman-Keuls post-hoc for comparison of dendritic arbor branching and length (in cases when the data was not normal we used a Kruskal Wallis one-way ANOVA on ranks with Dunn's method post-hoc), and a one-way ANOVA for comparison of spine density and morphology.

Results

Stroke size did not differ between the two stroke groups

Analysis of the stroke lesions in the Golgi-Cox stained tissue showed a mean size of approximately 22% of the intact contralateral hemisphere and included the sensorimotor cortex with minimal subcortical involvement (Fig. 1B, C). The size of the stroke lesion did not significantly differ between the stroke/control antibody group and the stroke/anti-Nogo-A antibody group (p=0.706; Fig. 1C).

Performance on the spatial reference memory task is improved in aged rats after stroke and treatment with anti-Nogo-A immunotherapy

Rats were tested over seven days in the place task, a spatial reference memory task. At the start of the place task animals in all groups found the hidden platform in a similar time frame ($p= 0.2122$; Fig. 1D, D'). As testing continued the rate at which rats in the stroke/anti-Nogo-A antibody group acquired the hidden platform location was faster than the stroke/control antibody group ($p<0.001$). In fact, the stroke/anti-Nogo-A antibody group was indistinguishable from the normal aged group ($p=0.1573$), while the rate at which the stroke/control antibody group acquired the hidden platform location was slower than the normal aged group ($p<0.001$). These findings were supported by analyzing the distance the rats took to locate the hidden platform. At the start of the place task animals in all groups swam similar distances to locate the platform ($p= 0.2122$; Fig. 1E, E'). As testing continued the rate at which rats in the stroke/anti-Nogo-A antibody group acquired the hidden platform location was faster than the stroke/control antibody group ($p<0.001$). However, both stroke groups had slower rates to acquire the hidden platform location than the normal aged group ($p<0.01$ for stroke/anti-Nogo-A antibody, $p<0.001$ for stroke/control antibody). Taken together, these results indicate that rats in the stroke/anti-Nogo-A antibody group acquired the hidden platform location faster than rats in the stroke/control antibody group.

At the completion of the place task, a probe trial was undertaken to assess if animals knew the former hidden platform location. All groups equally preferred the quadrant where the platform was previously located with no significant differences between groups ($p=0.876$; Fig. 1F). Additionally, there were no significant differences between groups in the number of times the rats swam over the location where the platform was previously located, i.e. "target visits" ($p = 0.858$; Supp. Fig. 2A). Therefore, at the end of the place task all groups had equally learned the hidden platform location.

Performance on a spatial working memory task is unaltered by stroke and antibody treatments

Following the probe trial, rats were tested on the matching-to-place task, a spatial working memory task. Rats in all groups found the platform faster on trial 2 than on trial 1 ($p<0.001$), and there were no significant differences between groups ($p=0.4387$ for trial 1, $p=0.0550$ for trial 2; Fig. 1G). Additionally, analyzing the data separately by trial across days revealed no significant differences between groups (Supp. Fig. 2B). Therefore, all groups performed equally well on the matching-to-place task and there was no apparent effects of stroke on spatial working memory.

Effects of stroke on behavior observed during the place task

Thigmotaxis was defined as swimming in the outer 50% of the pool area. At the start of the place task all groups swam similar times in the periphery of the pool ($p=0.1572$; Fig. 2A, A'). As testing continued both stroke groups significantly spent more time swimming in the periphery of the pool as compared to normal aged rats ($p<0.001$), and the two stroke groups were not significantly different from each other ($p=0.4028$). At the end of the place task all groups swam similar times in the periphery of the pool ($p=0.5220$). Thigmotaxis for distance showed similar results with the two stroke groups swimming significantly more distance in the periphery of the pool as compared to normal aged ($p<0.001$; Supp. Fig. 3). Therefore, rats with stroke regardless of treatment spent more time than normal aged rats in the periphery of the pool.

Path circuity is defined as the ratio of the direct distance to the platform/ the actual swim distance to the platform during a trial. Both stroke groups swam significantly less direct paths to the platform than normal aged rats ($p<0.05$; Fig. 2B), and the two stroke groups were not

significantly different from each other (p=1.00). Therefore, rats with stroke regardless of treatment took less direct paths to reach the platform, as compared to normal aged rats.

Swim velocities during the place task did not differ between groups (p=0.2476, Fig. 2C).

Dendritic complexity was slightly reduced in the hippocampus on the same side as the stroke in both stroke groups

Following behavioral testing and 13 weeks post-stroke, we examined the dendritic arbors of Golgi-Cox stained hippocampal CA3 and CA1 pyramidal cells and dentate gyrus granule cells (Fig. 3).

For CA3 pyramidal cells, first we compared the total number of branch segments and total dendritic length for the apical and basilar dendritic trees across groups. In CA3 pyramidal cell apical dendritic trees ipsilateral to the stroke both stroke groups had significant decreases as compared to normal aged rats in total number of branch segments ($p<0.001$), and total dendritic length ($p<0.05$; Fig. 4A). In CA3 pyramidal cell basilar dendritic trees ipsilateral to the stroke both stroke groups had significant decreases as compared to normal aged rats in total number of branch segments ($p<0.05$), but there were no significant differences in total dendritic length ($p=0.100$; Fig. 4B). Next we compared the number of branch segments and dendritic length of CA3 pyramidal cells by branch order across groups. In CA3 pyramidal cell apical dendritic trees ipsilateral to the stroke both stroke groups had significant decreases as compared to normal aged rats in number of branch segments (1^{st} , 2^{nd}, 4^{th}, 5^{th} orders, and 3^{rd} order only for stroke/control antibody), and dendritic length (0 order i.e. apical dendrite, and 1^{st} order; Fig. 4A'). In CA3 pyramidal cell basilar dendritic trees ipsilateral to the stroke both stroke groups had significant decreases as compared to normal aged rats in number of branch segments (3^{rd}, 4^{th} orders, and 1^{st} order only for stroke/control antibody), and dendritic length (4^{th} order; Fig. 4B').

For CA1 pyramidal cells, first we compared the total number of branch segments and total dendritic length for the apical and basilar dendritic trees across groups and there were no significant differences (Fig. 5A, B). Next we compared the number of branch segments and dendritic length of CA1 pyramidal cells by branch order across groups. In CA1 pyramidal cell apical dendritic trees ipsilateral to the stroke the stroke/control antibody rats had significant decreases as compared to normal aged rats in number of branch segments (1^{st} order; Fig. 5A'). In CA1 pyramidal cell basilar dendritic trees ipsilateral to the stroke the stroke/anti-Nogo-A antibody rats had significant decreases as compared to normal aged rats in dendritic length (2^{nd} order; Fig. 5B').

For dentate gyrus granule cells, first we compared the total number of branch segments and total dendritic length for the dendritic trees across groups and there were no significant differences (Fig. 6A). Next we compared the number of branch segments and dendritic length of dentate gyrus granule cells by branch order across groups. In dentate gyrus granule cell dendritic trees ipsilateral to the stroke the stroke/control antibody rats had significant decreases as compared to normal aged rats in number of branch segments (1^{st} order; Fig. 6A').

Therefore, there was a decrease in dendritic complexity on the same side as the stroke in CA3, CA1 and dentate gyrus neurons in both stroke groups.

Hippocampal dendritic spine density and morphology showed no differences between groups

Dendritic spine density of CA3 and CA1 pyramidal cell apical dendrites of second order or higher did not significantly differ between groups (Fig. 7A, C). When we analyzed number of dendritic spines by morphology there were no significant differences between groups for thin,

stubby and mushroom spines (Fig. 7B, D). Furthermore, there was no significant difference between groups for number of filopodia (Fig. 7B, D).

Discussion

The results from the present study show that anti-Nogo-A immunotherapy given one week following stroke in aged rats improved performance on the Morris water maze place task which was not correlated with anatomical changes in dendritic arbors of hippocampal CA3 and CA1 pyramidal, dentate gyrus granule cells or dendritic spines of CA3 and CA1 pyramidal cells. The results from the Morris water maze could potentially be confounded if the animals had gross motor deficits from the stroke lesion. However, no differences in swim velocity were detected between groups arguing against gross motor deficits as a confounding variable. By observation these animals did not appear to have motor deficits after stroke and they ambulated, fed, groomed and swam without difficulty. Furthermore, in our previous work we have shown that this stroke lesion in aged rats results in forelimb fine motor deficits which can only be demonstrated by a skilled reaching task [30].

For the matching-to-place task no significant differences were detected between groups, which in part could be due to the order of testing. During the place task the rats acquired procedural information about the Morris water maze such as there is no escape from the water at the wall of the pool, and that there is a platform to escape from the water always located in more central parts of the pool. The acquisition of this procedural information during the place task could have then affected the performance of the rats during the subsequent matching-to-place task. In particular the rats in the stroke/control antibody group may have benefited from the pre-existing procedural knowledge of the Morris water maze allowing them to perform as well as the normal aged rats and stroke/anti-Nogo-A antibody rats on the matching-to-place task.

Previous studies have shown that anti-Nogo-A immunotherapy, and the NgR(310)Ecto-Fc protein, which binds to the ligands of the Nogo-66 receptor (NgR) and thereby blocks receptor activation, are effective up to one week after stroke in rats in inducing recovery of sensorimotor function in the stroke-impaired forelimb [23,33,40-42]. Furthermore, improvement on a sensorimotor task has been shown in aged rats after stroke given anti-Nogo-A immunotherapy, although the recovery took longer to occur as compared to adult rats [30]. The sensorimotor recovery was correlated in adult rats with axonal sprouting from intact pathways across the midline into subcortical denervated areas [23,33,40,42], and dendritic sprouting and increased dendritic spine density in the contralesional sensorimotor cortex [34]. Further support for the role of Nogo-A in recovery from stroke is provided from genetic studies using knock-out models. Mice that lack the NgR or that lack Nogo-A and Nogo-B have improved sensorimotor recovery after a photothrombotic lesion to the sensorimotor cortex as compared to heterozygous littermates, and this correlates with axonal sprouting from intact pathways across the midline into the denervated red nucleus and spinal cord [23].

In the present study we show improved performance on a spatial memory task in aged rats after stroke and anti-Nogo-A immunotherapy given one week post-stroke. Several studies examining the therapeutic use of anti-Nogo-A immunotherapy to improve cognitive impairment in rodent brain injury models support our findings. In an experimental model of traumatic brain injury (TBI) adult rats that sustained a lateral fluid percussion injury and treatment with anti-Nogo-A immunotherapy starting 24 hours post-injury showed improved performance on the Morris water maze place task [24,29]. In that study, rats with TBI given anti-Nogo-A immunotherapy had a higher expression of growth-associated protein-43 (GAP-43) in CA1 of the hippocampus as compared to rats with TBI and treated with control antibody [29]. The higher levels of GAP-43 suggest that anti-Nogo-A immunotherapy may enhance the axonal growth potential of the hippocampus after TBI. Additionally, in a cortical

aspiration lesion model of severe neglect adult rats showed improvement from neglect when treated with anti-Nogo-A immunotherapy immediately following injury. These behavioral improvements could be abolished causing the rats to once again exhibit severe neglect by severing the corpus callosum, demonstrating the importance of the contralateral hemisphere in the behavioral recovery [5]. Interestingly, genetically modified unlesioned mice that lack Nogo-A have normal spatial memory on the Morris water maze, but have enhanced motor coordination and balance as compared to heterozygous littermates [43]. Our study adds to the growing body of literature of cognitive recovery with anti-Nogo-A immunotherapy by using the clinically relevant age group and time of treatment.

Due to the importance of the hippocampus for performance of spatial memory tasks [14], and the correlation of anti-Nogo-A immunotherapy with dendritic sprouting [34], we investigated whether the improved performance we found in the spatial reference memory task with anti-Nogo-A immunotherapy post-stroke would correlate with structural changes in the hippocampus. However, we found no differences in dendritic branching of CA3 and CA1 pyramidal and dentate gyrus granule cells, and no differences in spine density and morphology in CA3 and CA1 pyramidal cells between rats with stroke given anti-Nogo-A immunotherapy or given control antibody. This could be explained in several ways. First, morphological axonal or dendritic changes in brain areas other than the hippocampus may underlie the improved performance in the spatial memory task after anti-Nogo-A immunotherapy. Performance on the Morris water maze depends upon a distributed network of brain areas [14] that have neural activity in response to place including the medial entorhinal cortex, striatum, subiculum and lateral septum [22], areas which were not examined in this study. Interestingly, when rats received non-spatial pre-training to become familiar with the Morris water maze, blocking NMDA receptor-dependent long term potentiation (LTP) in the dentate gyrus did not result in impairment [39]. These studies suggest that, though the hippocampus is important for Morris water maze performance, other brain regions also contribute to performance on the Morris water maze. Secondly, although dendritic growth was examined quite extensively in CA3, CA1 and the dentate gyrus, we did not investigate axonal growth in the hippocampus raising the possibility that axonal growth may underlie the improved performance on the spatial memory task after anti-Nogo-A immunotherapy. Axonal growth in the hippocampus has been shown after treatment with anti-Nogo-A antibodies in cholinergic axons after damage to the septo-hippocampal pathway [7], and in hippocampal slice cultures either intact or after cutting the Schaffer collaterals [12], or perforant pathway [31]. Finally, we cannot rule out that non-morphological changes affecting factors such as electrophysiological characteristics or biochemical composition of hippocampal cells, or cells in other areas of the brain important for spatial memory may underlie the improved performance on the spatial memory task after anti-Nogo-A immunotherapy.

Previous studies have shown that unilateral MCAO impairs performance on the Morris water maze place task in adult [13,44] and aged rats [2], as we also show in our study. Aging alone also causes impaired performance on the Morris water maze place task [2,26]. Despite the consistent demonstration of impaired performance on the Morris water maze after unilateral MCAO by us and others and the importance of the hippocampus for performance on the Morris water maze, MCAO does not cause gross histological damage to the hippocampus [44]. Here we show a decrease in dendritic complexity in CA3, CA1 and dentate gyrus neurons of the ipsilesional hippocampus. One study of MCAO reported an increase in the NMDA receptor subunit NR2B mRNA in the ipsilesional dentate gyrus, an increase in synapsin II bilaterally in the dentate gyrus, and a decrease in NGFI-A mRNA bilaterally in CA3 as compared to naive animals [13], suggesting that unilateral MCAO can effect gene expression in the hippocampus. On the other hand another study found no significant differences in the CA1 subregion of the hippocampus in LTP, microtubule-associated 2 positive fibers, and glial fibrillary acidic protein (GFAP) positive cells between the contralesional and ipsilesional sides [32]. This study

found no changes in acetylcholine levels in the dorsal and ventral hippocampus in rats after MCAO as compared to sham operated rats and intact rats. Therefore, unilateral MCAO appears to cause some structural and gene expression changes in the hippocampus.

In this study we found that rats with stroke regardless of antibody treatment spent more time swimming near the wall of the pool, i.e. thigmotaxis, and took less direct routes to the platform during the place task than normal aged rats. This suggests rats with stroke are using different navigational strategies during the Morris water maze task. Thigmotaxis is considered a maladaptive behavior because the hidden platform is never located near the wall. Increases in thigmotaxis behavior have previously been reported after permanent MCAO [13,44], and in aged animals as compared to adult animals [2]. Yonemori et al. [44] reported that thigmotaxis behavior was correlated with shrinkage of the caudate-putamen, suggesting that damage to the caudate-putamen plays a role in thigmotaxis. Our method of MCAO results in a primarily cortical lesion with minimal damage to the underlying caudate-putamen [34]; however, it is possible that subtle damage to the caudate putamen underlies the thigmotaxis behavior we observed after stroke. These results suggest that although aged rats treated with anti-Nogo-A immunotherapy post-stroke are performing better on the Morris water maze than control antibody treated rats, they are not performing the task in the same manner as a non-stroke aged rat.

In conclusion, in the present study we found improved performance on the Morris water maze task after stroke and anti-Nogo-A immunotherapy in the aged, thereby providing further evidence that anti-Nogo-A immunotherapy may have potential as a treatment for cognitive impairment after stroke in the aged.

Supplementary Material

Refer to Web version on PubMed Central for supplementary material.

Acknowledgments

This work was supported by the Department of Veterans Affairs, NINDS grant 40960, NINDS grant F30NS060560, the Loyola University Chicago Neuroscience Institute, the Illinois Regenerative Medicine Institute, and the Swiss National Science Foundation. We thank Stephanie C. Johnson for help with the animals. We thank Novartis Pharma AG for the gift of the monoclonal antibodies.

References

[1]. Recommendations for Standards Regarding Preclinical Neuroprotective and Restorative Drug Development. Stroke 1999;30:2752–2758. [PubMed: 10583007]

[2]. Andersen MB, Zimmer J, Sams-Dodd F. Specific behavioral effects related to age and cerebral ischemia in rats. Pharmacol Biochem Behav 1999;62:673–682. [PubMed: 10208372]

[3]. Badan I, Buchhold B, Hamm A, Gratz M, Walker LC, Platt D, Kessler C, Popa-Wagner A. Accelerated glial reactivity to stroke in aged rats correlates with reduced functional recovery. J Cereb Blood Flow Metab 2003;23:845–854. [PubMed: 12843788]

[4]. Bourne JN, Harris KM. Balancing Structure and Function at Hippocampal Dendritic Spines. Annu Rev Neurosci 2008;31:47–67. [PubMed: 18284372]

[5]. Brenneman MM, Wagner SJ, Cheatwood JL, Heldt SA, Corwin JV, Reep RL, Kartje GL, Mir AK, Schwab ME. Nogo-A inhibition induces recovery from neglect in rats. Behav Brain Res 2008;187:262–272. [PubMed: 17963852]

[6]. Brown RW, Bardo MT, Mace DD, Phillips SB, Kraemer PJ. D-amphetamine facilitation of morris water task performance is blocked by eticlopride and correlated with increased dopamine synthesis in the prefrontal cortex. Behav Brain Res 2000;114:135–143. [PubMed: 10996054]

[7]. Cadelli D, Schwab ME. Regeneration of Lesioned Septohippocampal Acetylcholinesterase-positive Axons is Improved by Antibodies Against the Myelin-associated Neurite Growth Inhibitors NI-35/250. Eur J Neurosci 1991;3:825–832. [PubMed: 12106448]

[8]. Caroni P, Schwab ME. Antibody against myelin associated inhibitor of neurite growth neutralizes nonpermissive substrate properties of CNS white matter. Neuron 1988;1:85–96. [PubMed: 3272156]

[9]. Caroni P, Schwab ME. Two membrane protein fractions from rat central myelin with inhibitory properties for neurite growth and fibroblast spreading. J Cell Biol 1988;106:1281–1288. [PubMed: 3360853]

[10]. Chen MS, Huber AB, van der Haar ME, Frank M, Schnell L, Spillmann AA, Christ F, Schwab ME. Nogo-A is a myelin-associated neurite outgrowth inhibitor and an antigen for monoclonal antibody IN-1. Nature 2000;403:434–439. [PubMed: 10667796]

[11]. Clementz MA, Kanjanahaluethai A, O'Brien TE, Baker SC. Mutation in murine coronavirus replication protein nsp4 alters assembly of double membrane vesicles. Virology 2008;375:118–129. [PubMed: 18295294]

[12]. Craveiro LM, Hakkoum D, Weinmann O, Montani L, Stoppini L, Schwab ME. Neutralization of the membrane protein Nogo-A enhances growth and reactive sprouting in established organotypic hippocampal slice cultures. Eur J Neurosci 2008;28:1808–1824. [PubMed: 18973596]

[13]. Dahlqvist P, Ronnback A, Bergstrom SA, Soderstrom I, Olsson T. Environmental enrichment reverses learning impairment in the Morris water maze after focal cerebral ischemia in rats. Eur J Neurosci 2004;19:2288–2298. [PubMed: 15090055]

[14]. D'Hooge R, De Deyn PP. Applications of the Morris water maze in the study of learning and memory. Brain Res Brain Res Rev 2001;36:60–90. [PubMed: 11516773]

[15]. Gibb R, Kolb B. A method for vibratome sectioning of Golgi-Cox stained whole rat brain. J Neurosci Methods 1998;79:1–4. [PubMed: 9531453]

[16]. Glaser EM, Van der Loos H. Analysis of thick brain sections by obverse-reverse computer microscopy: application of a new, high clarity Golgi-Nissl stain. J Neurosci Methods 1981;4:117–125. [PubMed: 6168870]

[17]. Gonzenbach RR, Schwab ME. Disinhibition of neurite growth to repair the injured adult CNS: Focusing on Nogo. Cell Mol Life Sci 2008;65:161–176. [PubMed: 17975707]

[18]. GrandPre T, Nakamura F, Vartanian T, Strittmatter SM. Identification of the Nogo inhibitor of axon regeneration as a Reticulon protein. Nature 2000;403:439–444. [PubMed: 10667797]

[19]. Grotta JC, Jacobs TP, Koroshetz WJ, Moskowitz MA. Stroke Program Review Group: An Interim Report. Stroke 2008;39:1364–1370. [PubMed: 18309142]

[20]. Haines LM, O'Brien TE. Kurtosis and curvature measures for nonlinear regression models. Statistica Sinica 2004;14:547–570.

[21]. Kelly-Hayes M, Beiser A, Kase CS, Scaramucci A, D'Agostino RB, Wolf PA. The influence of gender and age on disability following ischemic stroke: the Framingham study. Journal of Stroke and Cerebrovascular Diseases 2003;12:119–126. [PubMed: 17903915]

[22]. Knierim JJ. Neural representations of location outside the hippocampus. Learn Mem 2006;13:405–415. [PubMed: 16882858]

[23]. Lee J-K, Kim J-E, Sivula M, Strittmatter SM. Nogo Receptor Antagonism Promotes Stroke Recovery by Enhancing Axonal Plasticity. J Neurosci 2004;24:6209–6217. [PubMed: 15240813]

[24]. Lenzlinger PM, Shimizu S, Marklund N, Thompson HJ, Schwab ME, Saatman KE, Hoover RC, Bareyre FM, Motta M, Luginbuhl A, Pape R, Clouse AK, Morganti-Kossmann C, McIntosh TK. Delayed inhibition of Nogo-A does not alter injury-induced axonal sprouting but enhances recovery of cognitive function following experimental traumatic brain injury in rats. Neuroscience 2005;134:1047–1056. [PubMed: 15979242]

[25]. Li S, Zheng J, Carmichael ST. Increased oxidative protein and DNA damage but decreased stress response in the aged brain following experimental stroke. Neurobiol Dis 2005;18:432–440. [PubMed: 15755669]

[26]. Lindner MD. Reliability, distribution, and validity of age-related cognitive deficits in the Morris water maze. Neurobiol Learn Mem 1997;68:203–220. [PubMed: 9398584]

[27]. Lloyd-Jones D, Adams R, Carnethon M, De Simone G, Ferguson TB, Flegal K, Ford E, Furie K, Go A, Greenlund K, Haase N, Hailpern S, Ho M, Howard V, Kissela B, Kittner S, Lackland D, Lisabeth L, Marelli A, McDermott M, Meigs J, Mozaffarian D, Nichol G, O'Donnell C, Roger V, Rosamond W, Sacco R, Sorlie P, Stafford R, Steinberger J, Thom T, Wasserthiel-Smoller S, Wong N, Wylie-Rosett J, Hong Y, for the American Heart Association Statistics Committee and Stroke Statistics Subcommittee. Heart Disease and Stroke Statistics--2009 Update: A Report From the American Heart Association Statistics Committee and Stroke Statistics Subcommittee. Circulation 2009;119:e21–181. [PubMed: 19075105]

[28]. Mar A, Spreekmeester E, Rochford J. Antidepressants preferentially enhance habituation to novelty in the olfactory bulbectomized rat. Psychopharmacology (Berl) 2000;150:52–60. [PubMed: 10867976]

[29]. Marklund N, Bareyre FM, Royo NC, Thompson HJ, Mir AK, Grady MS, Schwab ME, McIntosh TK. Cognitive outcome following brain injury and treatment with an inhibitor of Nogo-A in association with an attenuated downregulation of hippocampal growth-associated protein-43 expression. J Neurosurg 2007;107:844–853. [PubMed: 17937233]

[30]. Markus TM, Tsai SY, Bollnow MR, Farrer RG, O'Brien TE, Kindler-Baumann DR, Rausch M, Rudin M, Wiessner C, Mir AK, Schwab ME, Kartje GL. Recovery and brain reorganization after stroke in adult and aged rats. Ann Neurol 2005;58:950–953. [PubMed: 16315284]

[31]. Mingorance A, Fontana X, Sole M, Burgaya F, Urena JM, Teng FY, Tang BL, Hunt D, Anderson PN, Bethea JR, Schwab ME, Soriano E, del Rio JA. Regulation of Nogo and Nogo receptor during the development of the entorhino-hippocampal pathway and after adult hippocampal lesions. Mol Cell Neurosci 2004;26:34–49. [PubMed: 15121177]

[32]. Okada M, Nakanishi H, Tamura A, Urae A, Mine K, Yamamoto K, Fujiwara M. Long-term spatial cognitive impairment after middle cerebral artery occlusion in rats: no involvement of the hippocampus. J Cereb Blood Flow Metab 1995;15:1012–1021. [PubMed: 7593333]

[33]. Papadopoulos CM, Tsai S, Alsbiei T, O'Brien TE, Schwab ME, Kartje GL. Functional recovery and neuroanatomical plasticity following middle cerebral artery occlusion and IN-1 antibody treatment in the adult rat. Ann Neurol 2002;51:433–441. [PubMed: 11921049]

[34]. Papadopoulos CM, Tsai S-Y, Cheatwood JL, Bollnow MR, Kolb BE, Schwab ME, Kartje GL. Dendritic Plasticity in the Adult Rat Following Middle Cerebral Artery Occlusion and Nogo-A Neutralization. Cereb Cortex 2006;16:529–536. [PubMed: 16033928]

[35]. Paxinos, G.; Watson, C. The Rat Brain in Stereotaxic Coordinates. Academic Press; 2005.

[36]. Popa-Wagner A, Badan I, Walker L, Groppa S, Patrana N, Kessler C. Accelerated infarct development, cytogenesis and apoptosis following transient cerebral ischemia in aged rats. Acta Neuropathol 2007;113:277–293. [PubMed: 17131130]

[37]. Popa-Wagner A, Carmichael ST, Kokaia Z, Kessler C, Walker LC. The response of the aged brain to stroke: too much, too soon? Curr Neurovasc Res 2007;4:216–227. [PubMed: 17691975]

[38]. Prinjha R, Moore SE, Vinson M, Blake S, Morrow R, Christie G, Michalovich D, Simmons DL, Walsh FS. Inhibitor of neurite outgrowth in humans. Nature 2000;403:383–384. [PubMed: 10667780]

[39]. Saucier D, Cain DP. Spatial learning without NMDA receptor-dependent long-term potentiation. Nature 1995;378:186–189. [PubMed: 7477321]

[40]. Seymour AB, Andrews EM, Tsai SY, Markus TM, Bollnow MR, Brenneman MM, O'Brien TE, Castro AJ, Schwab ME, Kartje GL. Delayed treatment with monoclonal antibody IN-1 1 week after stroke results in recovery of function and corticorubral plasticity in adult rats. J Cereb Blood Flow Metab 2005;25:1366–1375. [PubMed: 15889044]

[41]. Tsai S-Y, Markus T, Andrews E, Cheatwood J, Emerick A, Mir A, Schwab M, Kartje G. Intrathecal treatment with anti-Nogo-A antibody improves functional recovery in adult rats after stroke. Exp Brain Res 2007;182:261–266. [PubMed: 17717658]

[42]. Wiessner C, Bareyre FM, Allegrini PR, Mir AK, Frentzel S, Zurini M, Schnell L, Oertle T, Schwab ME. Anti-Nogo-A antibody infusion 24 hours after experimental stroke improved behavioral outcome and corticospinal plasticity in normotensive and spontaneously hypertensive rats. J Cereb Blood Flow Metab 2003;23:154–165. [PubMed: 12571447]

[43]. Willi R, Aloy EM, Yee BK, Feldon J, Schwab ME. Behavioral characterization of mice lacking the neurite outgrowth inhibitor Nogo-A. Genes Brain Behav. 2008

[44]. Yonemori F, Yamaguchi T, Yamada H, Tamura A. Spatial cognitive performance after chronic focal cerebral ischemia in rats. J Cereb Blood Flow Metab 1999;19:483–494. [PubMed: 10326715]

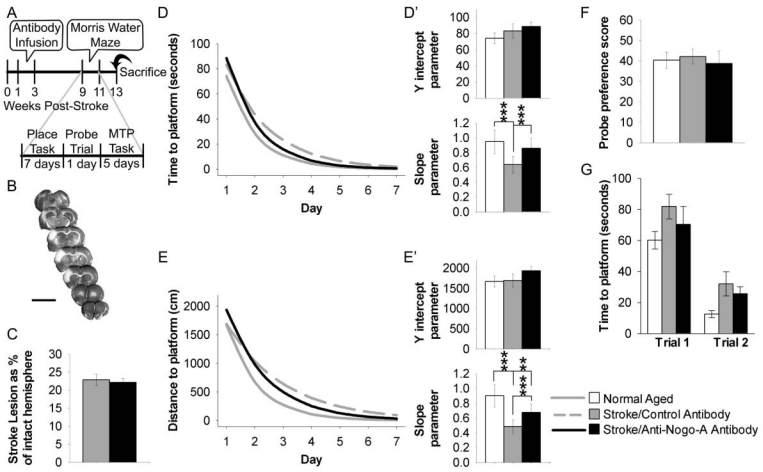

Figure 1.

Improved performance on a spatial reference memory task after stroke and treatment with anti-Nogo-A immunotherapy. (A) Timeline of experiments. (B) Representative right sided stroke lesion one day post-stroke in an aged rat (scale bar=1 cm). In the TTC (2,3,5-triphenyl-2H-tetrazolium chloride)-reacted coronal brain sections viable tissue appears red (shown here in gray) and the ischemic infarction appears white demonstrating sensorimotor cortex involvement and subcortical sparing. (C) The stroke lesion size quantified in Golgi-Cox stained tissue, represented as percent of the intact hemisphere, did not differ between the two stroke groups (p=0.706, t-test). (D) Time to locate the hidden platform during the Morris water maze place task. Average curves of the fitted functions for each group. (D') Averages of the individual parameters of the functions. Time at the start of testing, or the y intercept, was the same for all groups. As testing continued normal aged and stroke/anti-Nogo-A antibody treated rats acquired the location of the platform faster than stroke/control antibody treated rats, as shown by the slope parameter ($p < 0.001$, likelihood based $\chi 2$ test of random-effects simple exponential two-parameter model, $\eta(x) = \theta_1 e^{-\theta_2 x}$, where x = day – 1 [28]). (E) Distance to locate the hidden platform during the Morris water maze place task. Average curves of the fitted functions for each group. (E') Averages of the individual parameters of the functions. Distance at the start of testing, or the y intercept, was the same for all groups. As testing continued all three groups acquired the location of the platform at significantly different rates, with the stroke/anti-Nogo-A antibody treated rats having faster rates to acquire the platform location than stroke/control antibody treated rats ($p<0.001$ for stroke/anti-Nogo-A antibody and stroke/control antibody, $p<0.01$ for normal aged and stroke/anti-Nogo-A antibody, $p<0.001$ for normal aged and stroke/control antibody, likelihood based $\chi 2$ test of random-effects simple exponential two-parameter model, $\eta(x) = \theta_1 e^{-\theta_2 x}$, where x = day –1). (F) During the probe trial all groups equally preferred the quadrant that contained the platform during the place task (p=0.876, one-way ANOVA). (G) During the matching-to-place (MTP) task all groups found the platform faster on Trial 2 than on Trial 1 ($p<0.001$), and there were no significant differences between groups (p=0.4387 for trial 1, p=0.0550 for trial 2, one-way ANOVA). Error bars denote ± standard error of the mean. **p<0.01, ***p<0.001.

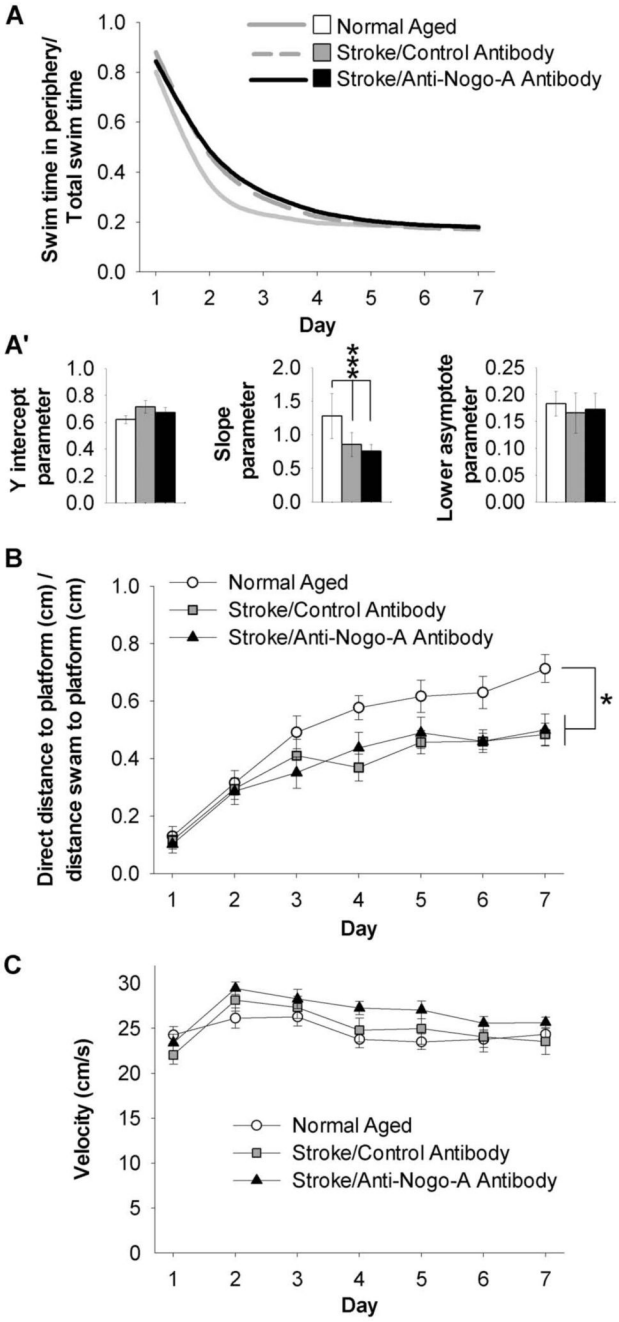

Figure 2.

Behaviors in the Morris water maze that were unique to rats with stroke regardless of antibody treatment. (A) Thigmotaxis, time spent in the periphery, during the place task. Average curves of the fitted functions for each group. (A') Averages of the individual parameters of the functions. Thigmotaxis at the start of testing, or the y intercept, was the same for all groups. As testing continued both stroke groups showed more thigmotaxis behavior than normal aged rats ($p<0.001$, likelihood based $\chi 2$ test of random-effects simple exponential three-parameter model, $\eta(x) = \theta_1 e^{-\theta 2x} + \theta_3$, where x = day – 1 [28]). Thigmotaxis at the end of testing, or the lower asymptote, was the same for all groups. (B) The path circuity or direct distance to the platform/ the actual distance swam to the platform during a trial during the place task. Both

stroke groups had significantly more circuitous paths than the normal aged group ($p<0.05$, repeated measures ANOVA, Bonferroni test for post-hoc comparison). (C) Swim velocity during the Morris water maze place task did not significantly differ across groups ($p=0.2476$, repeated measure ANOVA). Error bars denote ± standard error of the mean. *$p<0.05$, ***$p<0.001$.

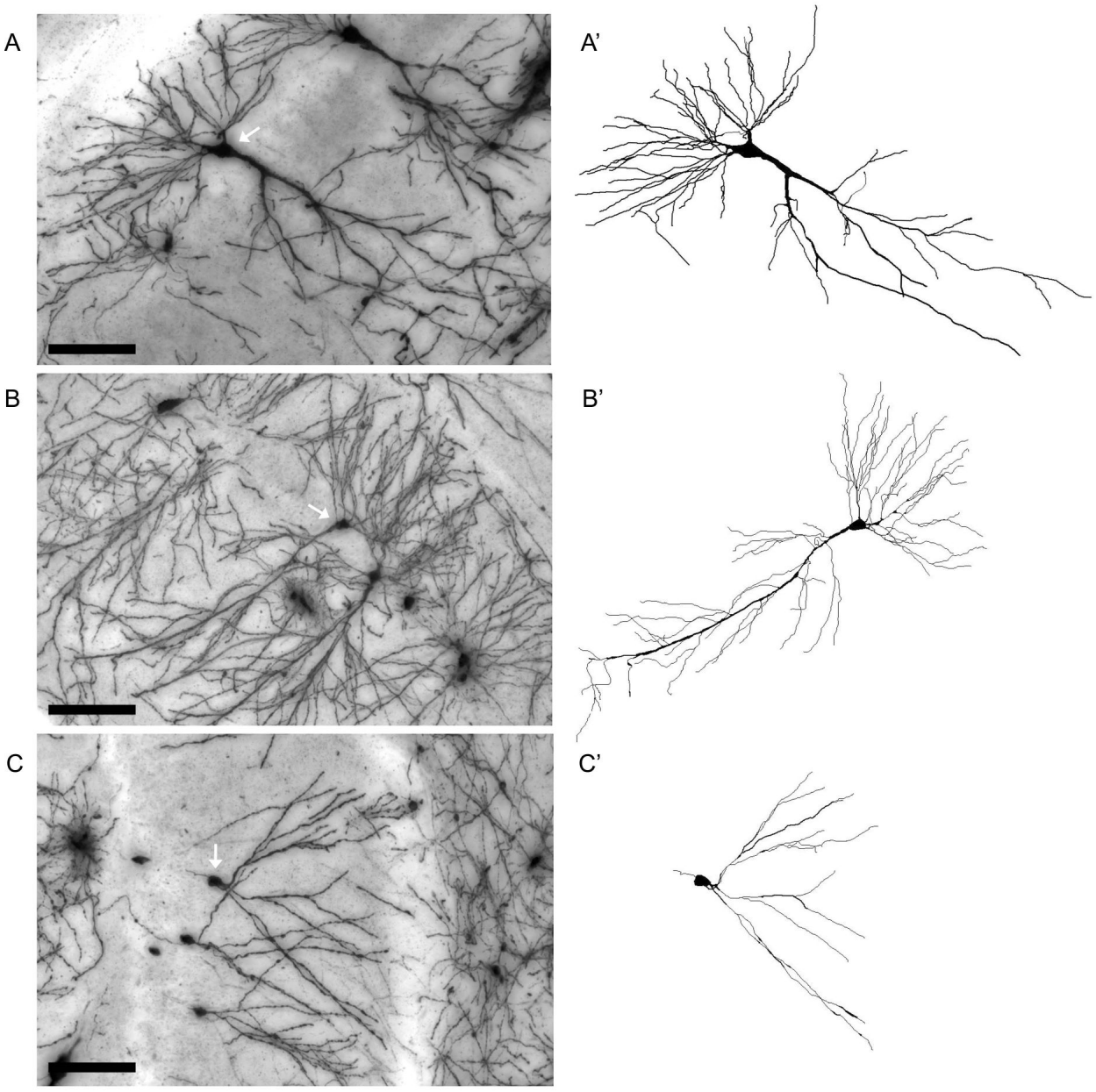

Figure 3.
Representative Golgi-Cox stained hippocampal CA3 (A) and CA1 pyramidal cells (B) and dentate gyrus granule cell (C, white arrows), and the corresponding Neurolucida tracings (A', B', C'). Images were acquired from the hippocampus of a normal aged rat. Scale bar=100 μm.

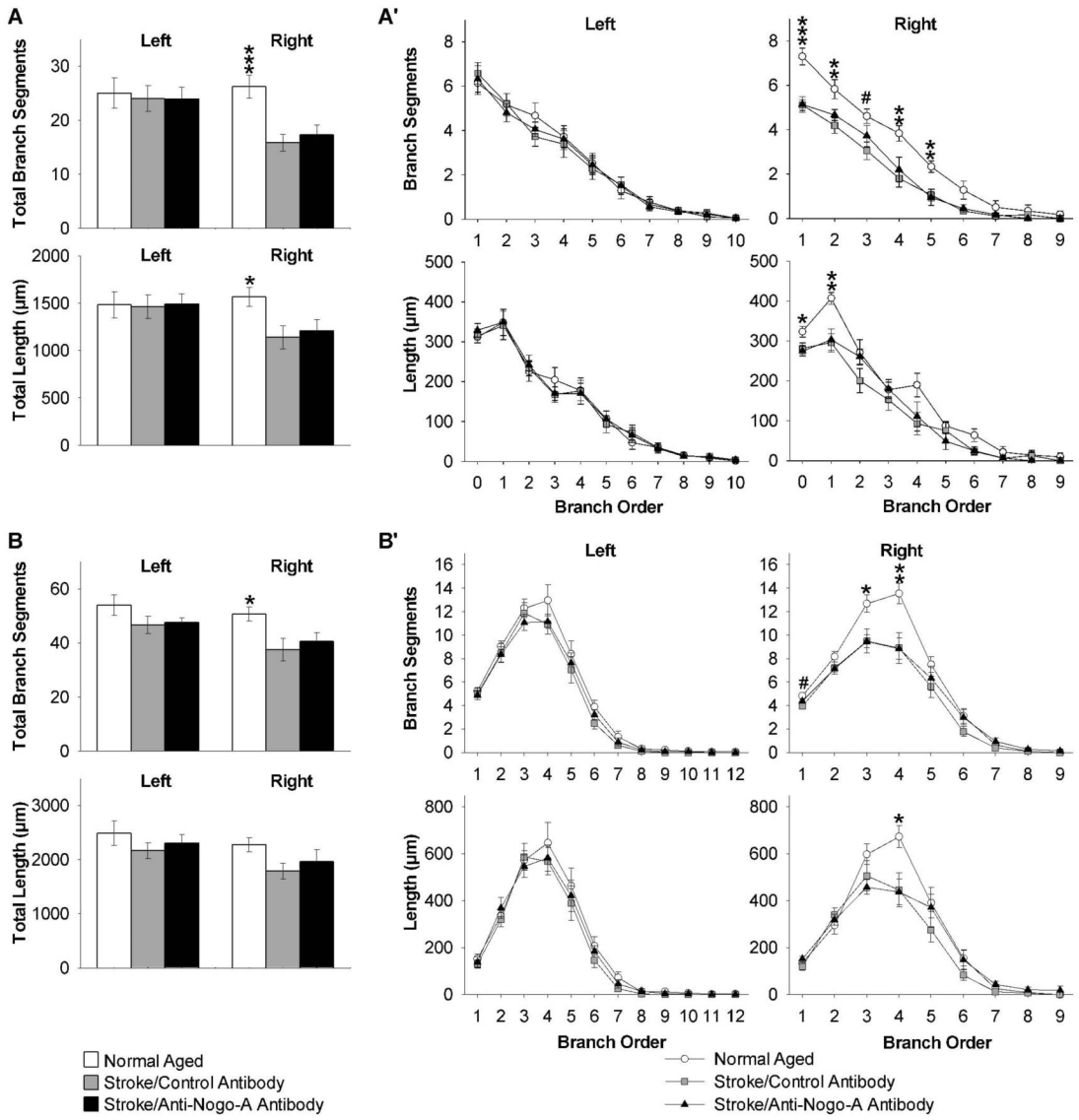

Figure 4.

Decreased dendritic arbor complexity of CA3 pyramidal cells in both stroke groups ipsilateral to the stroke (right). (A) Quantification of apical total number of branch segments and total dendritic length, and (A') apical branch segments and dendritic length in each branch order. (B) Quantification of basilar total number of branch segments and total dendritic length, and (B') basilar branch segments and dendritic length in each branch order. Error bars denote ± standard error of the mean. *p<0.05, ** p<0.01, ***p<0.001 for normal aged vs. both stroke groups, and #p<0.05 for normal aged vs. stroke/control antibody (one-way ANOVA p values reported, Student-Newman-Keuls test for post-hoc comparison).

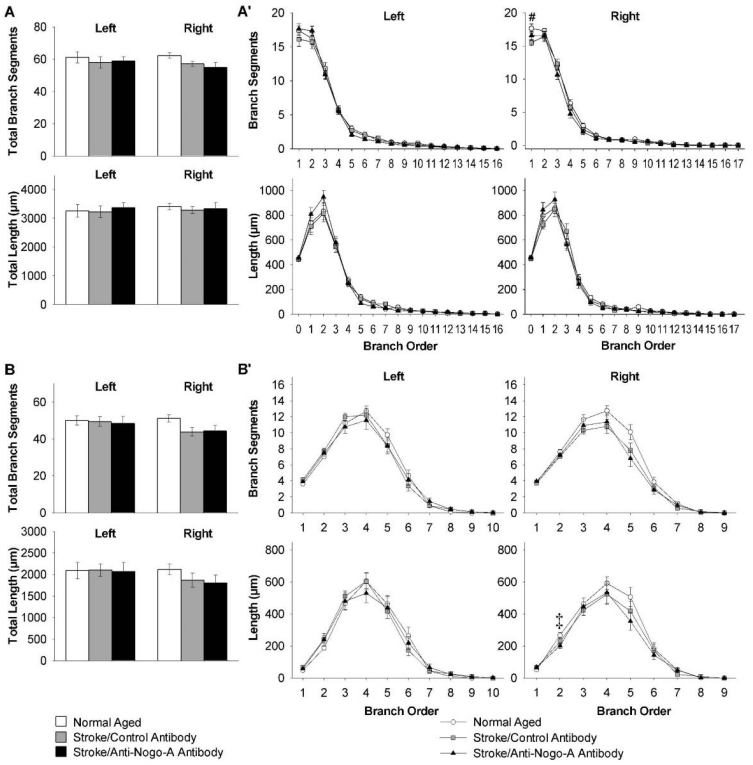

Figure 5.

Decreased dendritic arbor complexity of CA1 pyramidal cells in both stroke groups ipsilateral to the stroke (right). (A) Quantification of apical total number of branch segments and total dendritic length, and (A') apical branch segments and dendritic length in each branch order. (B) Quantification of basilar total number of branch segments and total dendritic length, and (B') basilar branch segments and dendritic length in each branch order. Error bars denote ± standard error of the mean. #$p<0.05$ for normal aged vs. stroke/control antibody (one-way ANOVA p value reported, Student-Newman-Keuls test for post-hoc comparison). ‡$p<0.05$ for normal aged vs. stroke/anti-Nogo-A antibody (Kruskal Wallis one-way ANOVA on ranks p value reported, Dunn's method for post-hoc comparison).

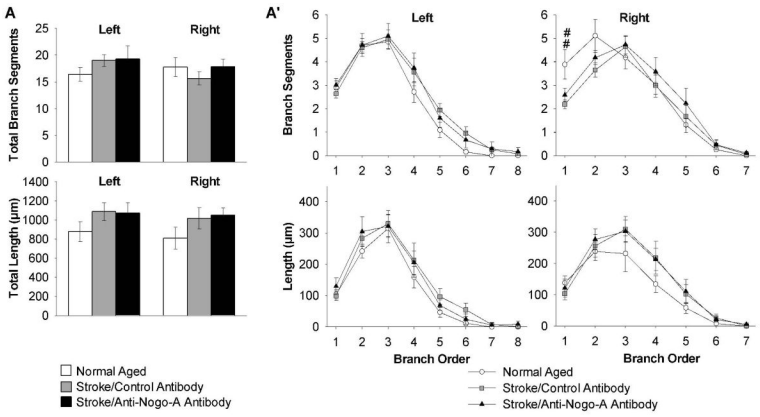

Figure 6.

Decreased dendritic arbor complexity of dentate gyrus granule cells in the stroke/control antibody group ipsilateral to the stroke (right). (A) Quantification of total number of branch segments and total dendritic length, and (A') branch segments and dendritic length in each branch order. Error bars denote ± standard error of the mean. ##$p<0.01$ for normal aged vs. stroke/control antibody (Kruskal Wallis one-way ANOVA on ranks p value reported, Dunn's method for post-hoc comparison).

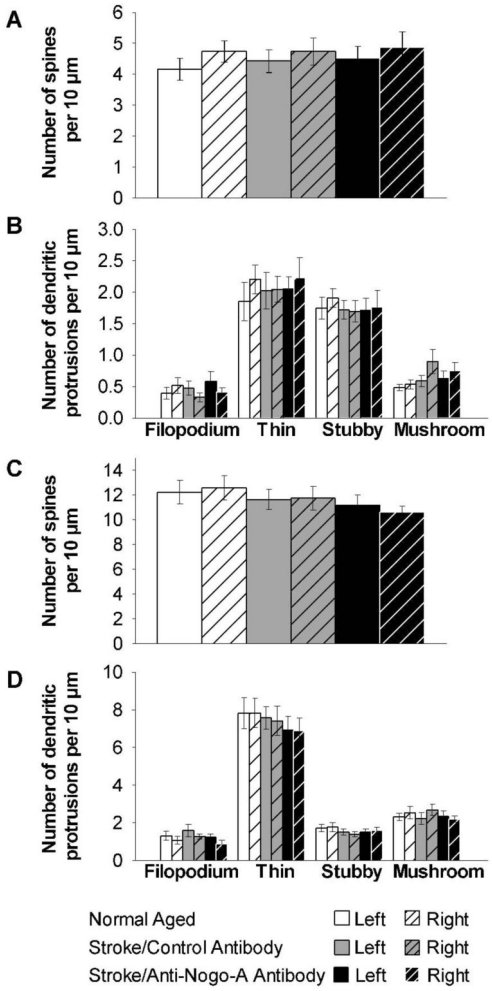

Figure 7.

Apical dendritic spine density and morphology in CA3 and CA1 pyramidal cells did not significantly differ across groups. (A) Quantification of CA3 pyramidal cell dendritic spine density, and (B) CA3 pyramidal cell dendritic protrusion morphology. (C) Quantification of CA1 pyramidal cell dendritic spine density, and (D) CA1 pyramidal cell dendritic protrusion morphology. Error bars denote ± standard error of the mean.